Exploring the Origin of Nearly Degenerate Doublet Bands in ^{106}Ag

N. Rather,[1] P. Datta,[2,*] S. Chattopadhyay,[1] S. Rajbanshi,[1] A. Goswami,[1] G. H. Bhat,[3] J. A. Sheikh,[3] S. Roy,[4] R. Palit,[4] S. Pal,[4] S. Saha,[4] J. Sethi,[4] S. Biswas,[4] P. Singh,[4] and H. C. Jain[4]

[1]*Saha Institute of Nuclear Physics, Kolkata 700064, India*

[2]*Ananda Mohan College, Kolkata 700009, India*

[3]*Department of Physics, University of Kashmir, Srinagar 190006, India*

[4]*Tata Institute of Fundamental Research, Mumbai 400005, India*

(Received 28 October 2013; revised manuscript received 16 April 2014; published 20 May 2014)

The lifetimes of the excited levels for the two nearly degenerate bands of ^{106}Ag have been measured using the Doppler-shift attenuation method. The deduced $B(E2)$ and $B(M1)$ rates in the two bands are found to be similar, except around the band crossing spin, while their moments of inertia are quite different. This is a novel observation for a nearly degenerate doublet band.

DOI: 10.1103/PhysRevLett.112.202503 PACS numbers: 27.60.+j, 21.10.Tg, 21.60.Ev

The effects of the shape of a finite fermion system on its collective modes of excitations remain a subject of intense research. This experimental evidence comes from different fields of research. For example, an ultracold cloud of $\sim 4 \times 10^5$ ^{6}Li atoms exhibits collective angular oscillation about a principal axis of the elliptic trap when the angle of the trap is suddenly rotated by $\sim 5°$ [1]. Another piece of evidence is the observation of strong dipole and quadrupole resonances in ultrasmall two-dimensional systems comprised of ~ 20 electrons per quantum dot [2,3], where the system can be described by an effective parabolic potential. However, the most well studied system of this class is the deformed atomic nucleus, which is a classic example of a quantum rotor. The angular momentum (I) and the corresponding energy (E) of the rotational levels are related as $E = AI(I+1)$, where A can be expressed in terms of an effective moment of inertia ($\Im$) defined by $A = \hbar^2/2\Im$. This concept of an average deformed shape for a system of a finite number of interacting nucleons is possible since the motions of the nucleons in a nucleus are fast compared to the rotational frequency. The systematic theoretical studies based on the deformed mean field potential (Nilsson potential) indicate that most of the deformed nuclei have an axially symmetric shape. For these nuclei, the collective rotation is possible only around an axis perpendicular to the symmetry axis. This rotational symmetry implies that the projection of the angular momentum on the symmetry axis (designated as K) is a conserved quantum number.

The extent of the quadrupole deformation (β_2) can be estimated by measuring the electric quadrupole transition rates $B(E2, I \rightarrow I-2)$ in the rotational band. However, such direct evidence for a generalized triaxial shape is not possible since the two deformation parameters, namely, β_2 and the extent of departure from the symmetric shape (γ), cannot be determined from a single experimental $B(E2)$ value. It should be noted that the triaxial shape breaks the rotational symmetry since the rotation is possible along any of the three principal axes. Although there is no direct evidence of a stable triaxial deformation in an atomic nucleus, there is a great deal of indirect spectroscopic evidence, such as signature inversion at high spins [4], a wobbling motion [5], and spin chirality [6]. In the case of spin chirality, the chiral symmetry is spontaneously broken in a triaxial nucleus due to the presence of the three orthogonal angular momenta of valence protons, valence neutrons, and the core [7]. The restoration of this broken symmetry in the laboratory frame leads to a pair of nearly degenerate rotational bands with the same parity. Thus, a pair of bands can be experimentally identified as chiral partners, provided that they exhibit nearly similar band structures, moments of inertia (MOI), and, more importantly, the transition probabilities [8]. Such situations have been best realized in ^{128}Cs [9] and ^{135}Nd [10] for the $A \sim 130$ region. In recent years, a number of doublet bands have also been reported in the $A \sim 100$ [11–14] region, but their band structures and MOI have been found to be different. In addition, the transition rates have not been measured. Thus, the origin of these bands of the $A \sim 100$ region could not be established. In the present work, we report the first precise measurement of transition rates in the doublet bands of ^{106}Ag.

In the previous work by Joshi *et al.* [12], it was proposed that the main and partner bands could arise due to the triaxial and the axially symmetric shapes, respectively, which was the reason for the observation of different MOI for the two bands. The origin of the shape transformation for the partner band was attributed to the chiral vibrations of the γ-soft ^{106}Ag. In a recent publication [15], Ma *et al.*. have proposed that these bands in ^{106}Ag may originate due to the two different quasiparticle structures, namely, $\pi(g_{9/2})^1 \otimes \nu(h_{11/2})^1$ for the main band and $\pi(g_{9/2})^1 \otimes \nu(h_{11/2})^3$ for the partner band. Thus, the previous investigations [12,15] on the origin of the doublet bands of ^{106}Ag have indicated two contrasting possibilities, namely, distinct shapes or distinct quasiparticle structures.

In order to resolve this issue and to get an insight into the origin of partner bands in the $A \sim 100$ region, the high-spin states of ^{106}Ag were populated through the ^{96}Zr (^{14}N, $4n$) reaction using a 68 MeV ^{14}N beam from the 14-UD Pelletron at Tata Institute of Fundamental Research (TIFR). In this reaction, ^{106}Ag was populated with about 21% of the total fusion evaporation cross section, as estimated from the projection angular-momentum coupled evaporation calculations [16]. The 1 mg/cm^2 thick enriched ^{96}Zr target had a ^{206}Pb backing of 9 mg/cm^2, which facilitated the measurement of the subpicosecond lifetimes for the high-spin levels of the main and the partner bands by using the Doppler-shift attenuation method. The γ rays were detected by the Indian National Gamma Array (INGA) [17], which consisted of 20 Compton suppressed clover detectors. The two- and higher-fold coincidence data were recorded in the fast digital data acquisition system based on Pixie-16 modules [18]. The time-stamped data were sorted in a γ-γ-γ cube and three angle-dependent γ-γ matrices with a time window of 150 ns using the multiparameter time-stamped based coincidence search (MARCOS) program, developed at TIFR.

There were 3.2×10^8 events in the cube which were analyzed using the RADWARE program LEVIT8R [19] to construct the level scheme of ^{106}Ag and to determine the relative intensities of the γ rays which do not exhibit any line shapes. The derived level structures for the doublet bands were found to be consistent with the reported level scheme [12]. The partner band was extended to $I^\pi = 21^-\hbar$ through the addition of a 767 keV $\Delta I = 1$ transition. The crossover $E2$ transition of 1500 keV was also observed. However, the interband transitions of 389 $(15^- \rightarrow 14^-)$ keV and 926 $(16^- \rightarrow 14^-)$ keV from the partner to the main band reported in the previous work were not observed.

The band structures of the doublet have been depicted in Fig. 1 through the $E(I)$ plot. It is observed from the figure that the moments of inertia of the two bands are quite different and that they crossed diabatically around $I = 14\hbar$. This crossing is a unique feature of ^{106}Ag among all the doublet bands reported in the $A \sim 100$ [12] region.

The transition rates for the levels of the doublet bands of ^{106}Ag were deduced from the level lifetime measurements. These subpicosecond lifetimes were measured using the Doppler-shift attenuation method. The line shapes were extracted from the angle-dependent γ-γ matrices, which were constructed by placing the gamma energies detected at a specific angle (40°, 90°, and 157°) along one axis while the coincident γ energy was placed on the other axis. The number of entries were 2.8×10^8, 3.5×10^8, and 3.9×10^8 for the 40°, 90°, and 157° matrices, respectively. The line shapes were observed in γ-gated spectra for both $E2$ and $M1$ transitions above $I^\pi = 12^-\hbar$ and $14^-\hbar$ for the main and partner bands, respectively. The sum gate of 376 $(10^- \rightarrow 9^-)$ keV and 343 $(11^- \rightarrow 10^-)$ keV transitions for the main band and 219 $(12^- \rightarrow 11^-)$ keV and 270 $(13^- \rightarrow 12^-)$ keV transitions for the partner band were

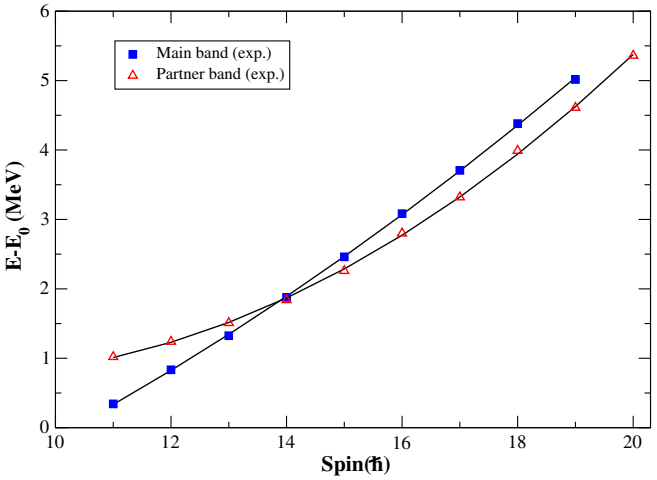

FIG. 1 (color online). The observed $E(I)$ plots for the doublet bands of ^{106}Ag. The energies are relative to the bandhead E_0 taken to be the energy of the $I^\pi = 10^-\hbar$ level of the main band. The solid line is a spline fit through the experimental data points.

used to extract the experimental line shapes in the respective bands. The relative intensities of these γ rays were obtained from the gated spectrum at 90°, which were normalized with the intensities of the transitions of the same multipolarity which have been estimated from the cube. The $B(M1)$-$B(E2)$ ratios obtained from the relative intensities for the two bands matched with the previously reported values [12] within $\pm 1\sigma$.

The lifetimes were measured by fitting the experimental line shapes at the forward and the backward angles simultaneously with the theoretical line shapes derived from the code LINESHAPE by Wells and Johnson [20]. The code was used to generate the velocity profiles of the recoiling nuclei at 40° and 157° with respect to the beam direction using the Monte Carlo technique with a time step of 0.001 ps for 5000 histories. The stopping power formula with shell correction of Northcliffe and Schilling [21] was used for calculating the energy loss of the recoiling ^{106}Ag nuclei in ^{206}Pb backing. The detailed procedure for line-shape fitting is described in Refs. [22,23].

For the main band, the effective lifetimes for the 18^- and 19^- levels were found by fitting the line shapes for 1309 $(19^- \rightarrow 17^-)$ keV and 1300 $(18^- \rightarrow 16^-)$ keV γ transitions by assuming a 100% sidefeed. The top feed lifetime for the 17^- level was assumed to be the intensity weighted average of the lifetimes for 18^- and 19^- levels since this level was fed by both 674 $(18^- \rightarrow 17^-)$ keV and 1309 keV γ rays. The sidefeeding intensity at this level was fixed to reproduce the observed intensity pattern at 90° with respect to the beam direction. In this way, each lower level was added one by one and fitted until all the observed line shapes for 1206 $(16^- \rightarrow 14^-)$ keV, 1146 $(15^- \rightarrow 13^-)$ keV, 1042 $(14^- \rightarrow 12^-)$ keV, and 979 $(13^- \rightarrow 11^-)$ keV γ rays were included into a global fit where only the in-band and feeding lifetimes were allowed

to vary. The uncertainties in the measured lifetimes were derived from the behavior of χ^2 in the vicinity of the minimum for the simultaneous fit at the two angles. The lifetime for the 12^- level was measured by fitting the line shape of the 833 $(12^- \rightarrow 10^-)$ keV γ ray extracted from the top gate of 490 keV. This was done to avoid the large feed to this level from other nonyrast states. In this case, the observed line shape was fitted by taking into account the complete top cascade, but no sidefeeding at the 12^- level was considered. In order to cross-check the consistency of the level lifetime measurements from the top and bottom gates in ^{106}Ag, the line shape of the 979 $(13^- \rightarrow 11^-)$ keV transition was extracted from the 552 $(14^- \rightarrow 13^-)$ keV gate and was fitted. The results from the top and bottom gates were found to agree within $\pm 1\sigma$.

All these levels also decay by $\Delta I = 1$ transitions, and their line shapes were fitted following the same prescription, except for the 490 $(13^- \rightarrow 12^-)$ keV and 489 $(12^- \rightarrow 11^-)$ keV γ rays since their line shapes overlapped. Thus, for most of the levels, the final values for the lifetimes were determined from the average of the values obtained from the independent fits to the two deexciting transitions. The corresponding uncertainty on a level lifetime has been calculated as the average of the uncertainties for the independent lifetime measurements for that level added in quadrature. However, it should be noted that the quoted errors do not include the systematic errors on the stopping power values, which may be as large as 20%.

In an earlier work by Levon *et al.*, the lifetimes of the low-spin levels from $8^-\hbar$ to $13^-\hbar$ of the main band of ^{106}Ag were measured using the recoil-distance Doppler-shift method [24]. The reported value of the lifetime for the 12^- level was 0.32(11) ps, which has been the same as obtained in the present work. However, the reported value of 0.39(14) ps for the 13^- level was probably the effective lifetime and thus did not match with the present work.

The same method of line-shape analysis was followed for the levels of the partner band. The 14^- level lifetime was extracted from the 326 keV $\Delta I = 1$ transition since the corresponding line shape of the crossover $E2$ transition of 597 keV could be contaminated due to the presence of a Ge$(n, n'\gamma)$ reaction. The intensity ratio of the interband to the intraband $\Delta I = 1$ transition for the 14^- level of the partner band was found to be 0.31(2). For the other levels whose lifetimes have been measured, the intensities of the interband $\Delta I = 1$ transitions could not be determined due to inadequate statistics in the 90° matrix. Examples of the line-shape fits in ^{106}Ag are shown in Fig. 2.

In order to deduce the $B(M1)$ rates from the measured level lifetimes, it was essential to estimate the mixing ratios (δ) for the $\Delta I = 1$ transitions. For the present fusion evaporation reaction, the width of the substate population σ/j was estimated to be 0.3 from the directional correlation of oriented nuclei (DCO) ratios of electric dipole and quadrupole transitions of ^{105}Ag. The mixing ratio for the

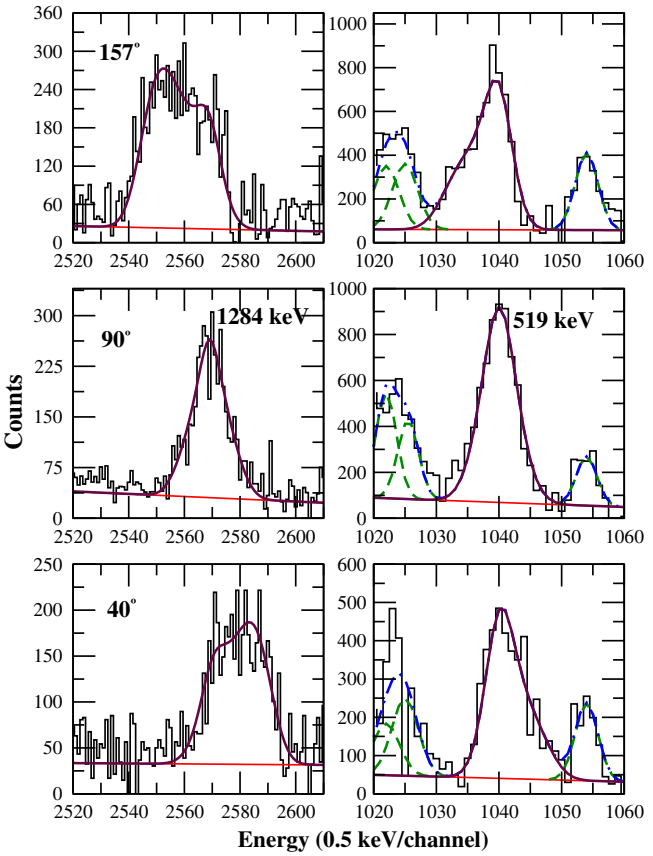

FIG. 2 (color online). Examples of the line-shape fits for the 1284 $(19^- \rightarrow 17^-)$ keV and 519 $(17^- \rightarrow 16^-)$ keV transitions at 40°, 90°, and 157° with respect to the beam direction. The Doppler broadened line shapes are drawn in solid lines, while the contaminant peaks are shown in dashed lines. The result of the fit to the experimental data is shown in dash-dotted lines.

$\Delta I = 1$ transitions were, then, estimated from the measured DCO values using $\sigma/j = 0.3$. These calculations were performed using the program ANGCOR [25]. It could be estimated that a 15% variation of the σ/j value leads to a 10% systematic error on the mixing ratios. The values of the mixing ratio, along with the level lifetime and the branching ratio for each level of the main and partner bands, have been tabulated in Table I. The uncertainties of the mixing ratios have been estimated by considering the extremum values of the uncertainties in the corresponding DCO values. It was found that the value of the mixing ratio doubles around the band crossing spin of $I = 14\hbar$. The $B(M1)$ and $B(E2, I \rightarrow I - 1)$ values of each level have been extracted from the corresponding level lifetime, branching, and mixing ratios. The uncertainties on the deduced rates were calculated from the quadrature addition of the individual uncertainties on the rates due to these three factors. For the three levels of the main band, whose mixing ratios were not estimated, the maximum possible value for the $B(M1)$ rates corresponded to $\delta = 0$ while the minimum possible value was estimated by assuming the maximum observed value for $\delta = 0.25(6)$. On the other hand, the

TABLE I. The measured lifetimes for the levels of the doublet bands, the corresponding mixing ratios, and the branching ratios of ^{106}Ag. The branching ratios are quoted for the $\Delta I = 1$ transitions. It should be noted that the quoted errors in the level lifetimes do not include the systematic errors in the stopping power values, which may be as large as 20%.

Spin $I(\hbar)$	Lifetime (ps)	Mixing ratio (δ)	Branching ratio $\frac{I_\gamma(\Delta I=1)}{I_\gamma(\text{total})}$
	Main band		
12^-	0.32(2)		0.84(7)
13^-	0.20(2)	0.12(5)	0.76(6)
14^-	0.23(2)	0.23(5)	0.61(5)
15^-	0.22(2)	0.25(6)	0.40(4)
16^-	0.17(1)		0.47(7)
17^-	0.10(1)		0.57(7)
	Partner band		
14^-	1.77(10)	0.09(4)	0.58(5)
15^-	0.31(3)	0.21(5)	0.87(7)
16^-	0.40(3)	0.24(3)	0.57(6)
17^-	0.27(2)	0.11(4)	0.45(5)
18^-	0.10(1)	0.14(7)	0.70(9)
19^-	0.11(1)	0.18(6)	0.36(5)

maximum and the minimum limits for the $B(E2, I \to I-1)$ values were found for $\delta = 0.25(6)$ and $\delta = 0$, respectively.

The deduced transition rates have been plotted in Fig. 3. It is observed from this figure that within the experimental uncertainties, all three transition rates for the two bands are essentially the same, except at $I = 15\hbar$, which probably originates due to the band crossing around this spin. The observation that the $B(E2, I \to I-2)$ are similar does not support the two different quasiparticle pictures of Ref. [15], since in that case, the rates in the partner band are expected to be 2 times stronger than that of the main band. However, the explanation based on two different shapes cannot be ruled out, since the measured $B(E2, I \to I-2)$ values for the main and partner bands can be reproduced by different sets of (β, γ) values.

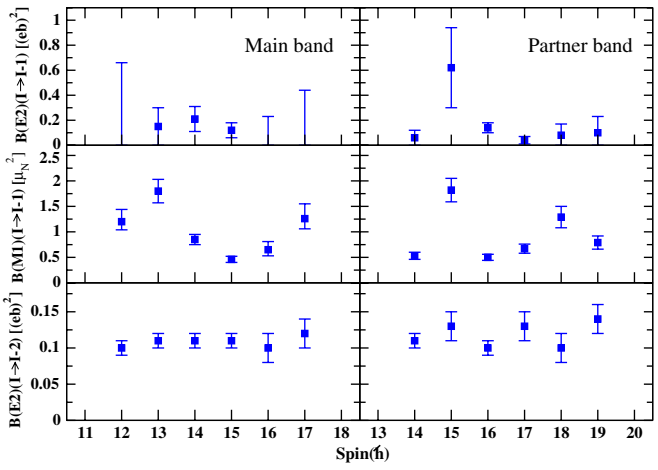

FIG. 3 (color online). The deduced $B(E2, I \to I-1)$, $B(M1, I \to I-1)$, and $B(E2, I \to I-2)$ rates for the doublet bands of ^{106}Ag.

Similar precise level lifetime measurements in nearly degenerate doublet bands had only been performed in the $A \sim 130$ region for ^{128}Cs [9], ^{135,136}Nd [10,26], and ^{134}Pr [27]. The MOI and transition rates were found to be very similar in ^{128}Cs and ^{135}Nd, which established that the doublet bands are chiral partners. On the other hand, the doublet bands of ^{134}Pr and ^{136}Nd exhibit the band crossing similar to that observed in ^{106}Ag. In both cases, the transition rates were found to be different and were interpreted within the frameworks of the interacting boson-fermion-fermion model and the tilted axis cranking model complemented by the random phase approximation. These calculations indicated that the dissimilar transition rates in the doublet bands of ^{136}Nd and ^{134}Pr may originate due to chiral vibration [26] and chiral fluctuation [27], respectively. However, in the present work, similar transition rates have been observed in the doublet bands of ^{106}Ag. This novel feature of different MOI but similar transition rates may contain a new physical insight into the origin of the doublet bands which are systematically observed in the transitional region of the nuclear chart.

The authors would like to thank the technical staff of the TIFR-BARC Pelletron Facility for its smooth operation throughout the experiment. The help and cooperation of members of the INGA Collaboration for setting up the array are acknowledged. This work was partially funded by the Department of Science and Technology, Government of India (No. IR/S2/PF-03/2003-III). N. R. and P. D. (Grant No. PSW-26/11-12) would also like to thank UGC for research support.

*Corresponding author.
pdatta.ehp@gmail.com

[1] M. J. Wright, S. Riedl, A. Altmeyer, C. Kohstall, E. R. Sánchez Guajardo, J. Hecker Denschlag, and R. Grimm, Phys. Rev. Lett. **99**, 150403 (2007).
[2] Ch. Sikorski and U. Merkt, Phys. Rev. Lett. **62**, 2164 (1989).
[3] T. Demel, D. Heitmann, P. Grambow, and K. Ploog, Phys. Rev. Lett. **64**, 788 (1990).
[4] I. Hamamoto, Phys. Lett. B **235**, 221 (1990).
[5] S. W. Ødegård *et al.*, Phys. Rev. Lett. **86**, 5866 (2001).
[6] S. Frauendorf, Rev. Mod. Phys. **73**, 463 (2001).
[7] V. I. Dimitrov, S. Frauendorf, and F. Donau, Phys. Rev. Lett. **84**, 5732 (2000); S. Frauendorf and J. Meng, Nucl. Phys. **A617**, 131 (1997).
[8] C. M. Petrache, G. B. Hagemann, I. Hamamoto, and K. Starosta, Phys. Rev. Lett. **96**, 112502 (2006).
[9] E. Grodner *et al.*, Phys. Rev. Lett. **97**, 172501 (2006).
[10] S. Mukhopadhyay *et al.*, Phys. Rev. Lett. **99**, 172501 (2007).

[11] C. Vaman, D. Fossan, T. Koike, K. Starosta, I. Lee, and A. Macchiavelli, Phys. Rev. Lett. **92**, 032501 (2004).
[12] P. Joshi, M. Carpenter, D. Fossan, T. Koike, E. Paul, G. Rainovski, K. Starosta, C. Vaman, and R. Wadsworth, Phys. Rev. Lett. **98**, 102501 (2007).
[13] P. Joshi *et al.*, Phys. Lett. B **595**, 135 (2004); J. Timar *et al.*, Phys. Lett. B **598**, 178 (2004); P. Joshi *et al.*, Eur. Phys. J. A **24**, 23 (2005).
[14] J. Sethi *et al.*, Phys. Lett. B **725**, 85 (2013).
[15] H.-L. Ma, S.-H. Yao, B.-G. Dong, X.-G. Wu, H.-Q. Zhang, and X.-Z. Zhang, Phys. Rev. C **88**, 034322 (2013).
[16] A. Gavron, Phys. Rev. C **21**, 230 (1980).
[17] S. Muralithar *et al.*, Nucl. Instrum. Methods Phys. Res., Sect. A **622**, 281 (2010).
[18] R. Palit *et al.*, Nucl. Instrum. Methods Phys. Res., Sect. A **680**, 90 (2012).
[19] D. C. Radford, Nucl. Instrum. Methods Phys. Res., Sect. A **361**, 297 (1995).
[20] J. C. Wells and N. R. Johnson, Oak Ridge National Laboratory Report No. ORNL-6689, 1991.
[21] L. C. Northcliffe and R. F. Schilling, At. Data Nucl. Data Tables **7**, 233 (1970).
[22] P. Datta *et al.*, Phys. Rev. C **69**, 044317 (2004).
[23] S. Roy *et al.*, Phys. Lett. B **694**, 322 (2011).
[24] A. I. Levon, J. de Boer, A. A. Pasternak, and D. A. Volkov, Z. Phys. A **343**, 131 (1992)
[25] E. S. Macias, W. D. Ruhtur, D. C. Camp, and R. G. Lanier, Comput. Phys. Commun. **11**, 75 (1976).
[26] S. Mukhopadhyay *et al.*, Phys. Rev. C **78**, 034311 (2008).
[27] D. Tonev *et al.*, Phys. Rev. Lett. **96**, 052501 (2006).